Computation algorithms for efficient coupled electromagnetic–thermal device simulation

J. Driesen, R. Belmans and K. Hameyer

Abstract: Coupled electromagnetic–thermal field problems using nonidentical finite-element meshes for the magnetic and thermal discretisation, as encountered for instance in the simulation of electromagnetic energy transducers such as motors and transformers, require the application of nonlinear iterative solution algorithms. The paper gives an overview of the commonly used weakly coupled block iterative Picard methods and relaxation techniques. Strongly coupled Newton methods, both with explicit and implicit Jacobian matrix computations are discussed. Local as well as global convergence issues are treated. In this respect, the use of an alternative continuation technique, the pseudotransient coupled algorithm, using transient calculations in the frequency domain by means of an envelope approach, is discussed. The performance of the algorithms is compared using representative benchmark problems with both moderate and strong interaction. This leads to indications and a choice table on how to select appropriate algorithms for these coupled problems.

1 Introduction

Electrical energy transducers, such as transformers and electromagnetic actuators, exhibit different behaviour when their internal temperature distribution changes, mainly due to temperature-dependent electromagnetic material characteristics. For instance, permanent magnets change their operating characteristics and the conductivity of the winding/bar material drops at elevated temperature [1]. The thermal sources involved are dominated by conductive and iron losses. Similar effects take place in electroheat applications, for instance induction heating devices. This electromagnetic–thermal field interaction needs to be modelled using a coupled problem approach [2, 3]. Here, mainly low-frequency applications are considered, but similar problems exist for high-frequency devices [4].

Mathematically, coupled electromagnetic–thermal problems are mutually nonlinearly-dependent physical field problems. Many algorithms can theoretically solve these types of nonlinear equation systems [5]. Here, they are discussed using a generally coupled electromagnetic–thermal field problem, indicated as

$$\begin{cases} \mathbf{G}_A(\mathbf{A}, \mathbf{T}') = \mathbf{0} \\ \mathbf{G}_T(\mathbf{A}', \mathbf{T}) = \mathbf{0} \end{cases} \tag{1}$$

with $\mathbf{G}_A$ the field equation describing the magnetic field in terms of the vector potential $\mathbf{A}$. The second dependent variable $\mathbf{T}'$ is required to include the temperature dependence of some terms in the equations. $\mathbf{G}_T$ represents the thermal field equation in terms of the temperature $\mathbf{T}$. Here, the second dependent variable $\mathbf{A}'$ is needed to include the electromagnetic loss densities. The accent used in the mutually interacting variables indicates that a projection operation is required to transfer the solution between the different solution domains of the associated subproblems. (1) can represent a steady-state as well as a transient problem. As (1) is a set of nonlinear equations, a unique solution is not guaranteed. Therefore it is possible that more than one mathematical solution exists, especially in the case of uncontrolled extrapolation of the material characteristics as this does not always yield physically consistent situations.

2 Coupled field equations

Usually the finite-element method (FEM) is used to numerically compute such interacting fields. It is often required to employ different meshes as all regions do not have the same physical properties. For example, the air surrounding an electrical motor, carrying part of the leakage field, is meshed for the magnetic field whereas it can be replaced by a convection boundary condition for the thermal problem definition. The projection producing the discretised $\mathbf{A}'$ and $\mathbf{T}'$ field, starting from the differently discretised $\mathbf{A}$ and $\mathbf{T}$ field is an explicit interpolation or a best-fit calculation, the latter yielding a problem to solve on its own as it represents a least-squares fit of the solution written in terms of the other mesh's basis functions, to the known solution.

A generally coupled electromagnetic–thermal coupled problem in 2D is described by

$$\nabla \cdot (\upsilon_r \nabla(\mathbf{A})) - \mu_0 \sigma(\mathbf{T}') \frac{\partial \mathbf{A}}{\partial t} = -\mu_0 \sigma(\mathbf{T}') \frac{V_s}{L} \tag{2}$$

$$\nabla \cdot (\lambda \nabla \mathbf{T}) - \rho c \frac{\partial \mathbf{T}}{\partial t} = -q_J(\mathbf{T}, \mathbf{A}') \tag{3}$$

The first equation gives the magnetic field for a device with length L, supplied by voltage source V_s with reluctivity υ_r, thermal conductivity λ, mass density ρ and specific heat c, containing a temperature dependent electrical conductivity σ. The heat sources are limited to the Joule losses. Further interactions may be due to iron losses, temperature-dependent magnetic characteristics or other dependencies.

IEE Proceedings online no. 20020155

DOI: 10.1049/ip-smt:20020155

Paper first received 13th June 2001 and in revised form 10th January 2002

The authors are with the Dept. EE (ESAT), Div. ELEN, Katholieke Universiteit Leuven, Kasteelpark Arenberg 10, Heverlee B-3001, Belgium

These have been left out for simplicity, but their treatment is similar.

In an oscillating steady-state situation, e.g. under AC supply conditions, a frequency-domain method may be more appropriate for the magnetic field solution, describing the field by means of phasors $\mathbf{A}$ and V_s:

$$\nabla \cdot (\upsilon_r \nabla \underline{\mathbf{A}}) - \mu_0 \sigma(\mathbf{T}') j\omega \underline{\mathbf{A}} = -\mu_0 \sigma(\mathbf{T}') \frac{\underline{V_s}}{L} \tag{4}$$

$$\nabla \cdot (\lambda \nabla \mathbf{T}) = -q_J(\mathbf{T}, \underline{\mathbf{A}}') \tag{5}$$

(4) is obtained from (2) using

$$\mathbf{A}(t) = \underline{\mathbf{A}} \cdot e^{j\omega t} \tag{6}$$

The transient simulation (2) and (3) shows a major difficulty: the numerical stiffness due to the large ratio of the typical electromagnetic (very small) and thermal time constants (very large) involved. In such cases, a simulation with large time steps is still desired, but far from obvious.

An often-made approximation consists of the combination of the steady-state (4), approximating the s lowly changing overall magnetic field pattern by omitting the second derivative in (7), and the transient thermal (3).

$$\frac{d\mathbf{A}}{dt} = \left(j\omega \underline{\mathbf{A}} + \frac{\partial \underline{\mathbf{A}}}{\partial t} \right) e^{j\omega t} \tag{7}$$

However, this approximation implicitly holds an extrapolation of, for instance, the losses, yielding divergence for particular technical models. This is explained by the error in the heat sources, calculated as if the system were at steady state, that are systematically wrong, yielding overrated losses in most practical cases. In such a case, it is better to include the entire expression of (7) and assume that the phasor $\mathbf{A}$ evolves in time at the rate of the slower thermal time constants. This yields a transient frequency-domain method or envelope calculation method [6], allowing a more stable simulation of the magnetic field changes at large time-steps

$$\nabla \cdot (\upsilon_r \nabla \underline{\mathbf{A}}) - \mu_0 \sigma(\mathbf{T}') \left(j\omega \underline{\mathbf{A}} + \frac{\partial \underline{\mathbf{A}}}{\partial t} \right) = -\mu_0 \sigma(\mathbf{T}') \frac{\underline{V_s}}{L} \tag{8}$$

The interpretation of this approach is clarified in Fig. 1. The slowly changing envelope evolves with far less dynamics than the underlying oscillating function. This approach has also been suggested to solve circuit problems with largely different frequencies involved, for instance in mixer circuits [7–10].

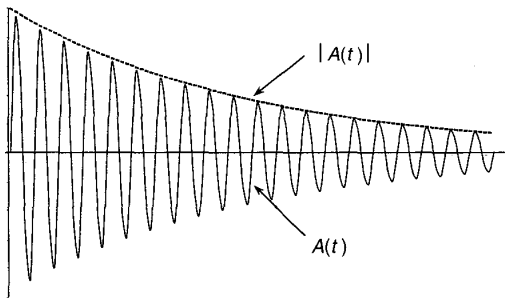

Fig. 1 *Graphical interpretation of the solution envelope*

3 Overview of coupled-field solution methodologies

The solution algorithms to solve the general nonlinear coupled problem (1) are iterative and can be distinguished in two categories [5].

3.1 Picard algorithms

The Picard algorithms or weakly-coupled successive substitution methods consist of iterating over a sequence (cascade) of more or less standard subproblem solutions. The intermediate operations contain loss-calculation algorithms and the calculation of the thermal influence on the relevant local material characteristic, featuring as a dependent coefficient. Possibly different subproblem meshes are combined, using separate projection operations in between calculations.

When the partial solutions are immediately re-used, a sequential block Gauss–Seidel algorithm is obtained

$$\begin{cases} \mathbf{A}^{(k+1)} = \mathbf{H}_A\left(\mathbf{A}^{(k)}, \mathbf{T}'^{(k)}\right) \\ \mathbf{T}^{(k+1)} = \mathbf{H}_T\left(\mathbf{A}'^{(k+1)}, \mathbf{T}^{(k)}\right) \end{cases} \tag{9}$$

Otherwise, a block Jacobi algorithm that can be parallelised is applicable. In these algorithms only function evaluations and field solutions, represented by $\mathbf{H}_A$ and $\mathbf{H}_T$, have to be calculated. Therefore these types of methods are commonly used [3], as it allows the re-use of individual field solvers within a computation shell.

3.2 Newton algorithms

Theoretically, Newton algorithms are a more interesting choice to solve nonlinear problems as they promise a quadratic convergence when close to the exact solution. Therefore it is interesting to consider whether it is possible and worth implementing.

3.2.1 Newton–Raphson algorithm: In the Newton–Raphson method a set of corrections δ_A and δ_T, to be added to an approximation or estimate of the entire nonlinear solution, is calculated [2, 3, 11]. The Jacobian matrix, containing all first-order derivatives and system residuals, evaluated in the estimated solution, is present in the large jacobian 'correction' equation containing all field variables at the same time (here, the arguments of the nonlinear residuals in (1) are omitted to simplify the notation)

$$\begin{bmatrix} \dfrac{\partial \mathbf{G}_A}{\partial A} & \dfrac{\partial \mathbf{G}_A}{\partial T'} \cdot \dfrac{\partial T'}{\partial T} \\ \dfrac{\partial \mathbf{G}_T}{\partial A'} \cdot \dfrac{\partial A'}{\partial A} & \dfrac{\partial \mathbf{G}_T}{\partial T} \end{bmatrix} \cdot \begin{bmatrix} \delta_A \\ \delta_T \end{bmatrix} = -\begin{bmatrix} \mathbf{G}_A \\ \mathbf{G}_T \end{bmatrix} \tag{10}$$

However, in the case of a frequency-domain method with complex variables, $\mathbf{G}_A$ should be in an analytic form to calculate the jacobian elements as such [12]. The necessary conditions are

$$\frac{\partial \mathrm{Re}\{\mathbf{G}_A\}}{\partial \mathrm{Re}\{A\}} = \frac{\partial \mathrm{Im}\{\mathbf{G}_A\}}{\partial \mathrm{Im}\{A\}}, \quad \frac{\partial \mathrm{Re}\{\mathbf{G}_A\}}{\partial \mathrm{Im}\{A\}} = -\frac{\partial \mathrm{Im}\{\mathbf{G}_A\}}{\partial \mathrm{Re}\{A\}} \tag{11}$$

These are not fulfilled, as for instance indicated in [12], and as a consequence the derivatives cannot be determined directly. Then, the system has to be split into a real and

imaginary component, complicating and enlarging the system

$$\begin{bmatrix} \frac{\partial \mathrm{Re}\{\mathbf{G}_A\}}{\partial \mathrm{Re}\{A\}} & \frac{\partial \mathrm{Re}\{\mathbf{G}_A\}}{\partial \mathrm{Im}\{A\}} & \frac{\partial \mathrm{Re}\{\mathbf{G}_A\}}{\partial T'} \cdot \frac{\partial T'}{\partial T} \\ \frac{\partial \mathrm{Im}\{\mathbf{G}_A\}}{\partial \mathrm{Re}\{A\}} & \frac{\partial \mathrm{Im}\{\mathbf{G}_A\}}{\partial \mathrm{Im}\{A\}} & \frac{\partial \mathrm{Im}\{\mathbf{G}_A\}}{\partial T'} \cdot \frac{\partial T'}{\partial T} \\ \frac{\partial \mathbf{G}_T}{\partial \mathrm{Re}\{A'\}} \cdot \frac{\partial \mathrm{Re}\{A'\}}{\partial \mathrm{Re}\{A\}} & \frac{\partial \mathbf{G}_T}{\partial \mathrm{Im}\{A'\}} \cdot \frac{\partial \mathrm{Im}\{A'\}}{\partial \mathrm{Im}\{A\}} & \frac{\partial \mathbf{G}_T}{\partial T} \end{bmatrix} \times \begin{bmatrix} \mathrm{Re}\{\delta_A\} \\ \mathrm{Im}\{\delta_A\} \\ \delta_T \end{bmatrix} = - \begin{bmatrix} \mathrm{Re}\{\mathbf{G}_A\} \\ \mathrm{Im}\{\mathbf{G}_A\} \\ \mathbf{G}_T \end{bmatrix} \tag{12}$$

The extra derivative factors in the off-diagonal blocks of (10) and (12) are due to the projection expressions. This and the many dependabilities yield an increased fill-in of the sparse jacobian. In many cases the explicit determination of the partial derivatives is a major problem as, for instance, the losses are computed through a complicated procedure and the material data are represented by look-up tables.

The advantage of this Newton–Raphson method is that it will converge very quickly in the vicinity of the exact solution. However, the block-structured jacobians in (9) and (11) are asymmetrical and realistic problems which often exhibit a high condition number [11], owing to the different nature of the underlying parameters. Therefore expensive iterative linear system solvers such as GMRES [13] (in practice used in the restarted version) are required. Another disadvantage is the fact that (12) becomes an extremely large equation to solve, where the main difficulty is the construction of a suitable preconditioning method.

3.2.2 Quasi-Newton algorithms: The computational cost of a Newton–Raphson method is obviously twofold. First, it is determined by the effort required for the construction of the jacobian and, next, the solution of the correction equation system. To avoid this burden, many approximations or quasi-Newton methods have been proposed that often try to approximate the jacobian matrix, e.g. by keeping it fixed for a few iterations [14]. An interesting alternative in this respect is to approximate the product of the jacobian $\mathbf{J}$ and a vector $\mathbf{v}$, with a small norm [14, 15]. This type of matrix–vector product is found in transpose-free iterative linear system solvers such as GMRES (generalised minimal residual method) or QMR-based methods [13]. The approximation consists of the use of the difference of the operating point (partial) residual and a perturbed (partial) residual

$$\mathbf{J}(\mathbf{x}_j) \cdot \mathbf{v} \simeq \frac{\mathbf{G}_i(\mathbf{x}_j + \kappa \mathbf{v}) - \mathbf{G}_i(\mathbf{x}_j)}{\kappa} \tag{13}$$

In practice, only the perturbed residual part has to be calculated, requiring the solution of the considered field problem, though with a good starting solution, particularly in the previous approximation. The other term is in fact the operating-point residual, initially computed for the right-hand side of the jacobian equation system. Hence, a so-called jacobian matrix-free algorithm or 'implicit jacobian' method is obtained. Obviously, the accuracy of the approximation depends on the choice of κ. It influences the approximation as well as the round-off errors. A good choice [14, 15] is

$$\kappa = 2\varepsilon^{1/2} \max\left(|x_j|, magn(x_j)\right) \|\mathbf{v}\|^{-1/2} \tag{14}$$

However, to use the difference approximation (13) along with the jacobian in (10), several evaluations of a residual part (in practice an individual field solution), at least one for every subproblem block, are required. An advantage is that they can be executed in parallel. In this way the first computational problem of the Newton approach, the construction of the jacobian, is avoided, but the GMRES algorithm will still result in high memory consumption. Therefore it is often more interesting to rewrite the equations explicitly in terms of a smaller set of variables, the 'coupling variables' [11]. Here, the set of electrical conductivities and loss quantities connected to the finite-element mesh is appropriate

$$\begin{cases} \mathbf{q} - G_q(\boldsymbol{\sigma}) = \mathbf{0} \\ \boldsymbol{\sigma} - G_\sigma(\mathbf{q}) = \mathbf{0} \end{cases} \tag{15}$$

Then, the jacobian equation becomes

$$\begin{bmatrix} \mathbf{I} & -\frac{\partial \mathbf{G}_q}{\partial \sigma} \\ -\frac{\partial \mathbf{G}_\sigma}{\partial q} & \mathbf{I} \end{bmatrix} \cdot \begin{bmatrix} \boldsymbol{\delta}_q \\ \boldsymbol{\delta}_\sigma \end{bmatrix} = - \begin{bmatrix} \mathbf{q}^* - \mathbf{G}_q(\boldsymbol{\sigma}^*) \\ \boldsymbol{\sigma}^* - \mathbf{G}_\sigma(\mathbf{q}^*) \end{bmatrix} \tag{16}$$

Using the difference approximation (13), the jacobian–vector product in the GMRES procedure reduces to (16). The calculation of the perturbed partial residuals can be performed in parallel. The operation-point solution is a good starting point of this calculation

$$\begin{bmatrix} \mathbf{I} & -\frac{\partial \mathbf{G}_q}{\partial \sigma} \\ -\frac{\partial \mathbf{G}_\sigma}{\partial q} & \mathbf{I} \end{bmatrix} \cdot \begin{bmatrix} \mathbf{v}_q \\ \mathbf{v}_\sigma \end{bmatrix} \simeq \begin{bmatrix} \mathbf{v}_q + \frac{\mathbf{G}_q(\boldsymbol{\sigma}^*) - G_q(\boldsymbol{\sigma}^* + \kappa_\sigma \mathbf{v}_\sigma)}{\kappa_\sigma} \\ \mathbf{v}_\sigma + \frac{\mathbf{G}_\sigma(\mathbf{q}^*) - G_\sigma(\mathbf{q}^* + \kappa_q \mathbf{v}_q)}{\kappa_q} \end{bmatrix} \tag{17}$$

This variable reduction could have been applied also to the traditional Newton approach, but in that case the difficulties encountered while deriving the jacobian elements would have increased dramatically owing to the complex interdependencies in this equation system. The result would be a very dense jacobian.

4 Global convergence issues

The Picard or Newton methods possess good local convergence properties in the vicinity of the exact solution. Therefore a good starting solution is a prerequisite. If a good estimate is not (yet) available, for example at the beginning of the computation, additional measures have to be taken to ensure the global convergence. Two interesting techniques can be used.

4.1 Adaptive relaxation

A relaxation technique damps the corrections calculated in an iterative step. To obtain a reasonable convergence rate, these parameters can be adapted in every iteration step by estimating nearly optimal damping coefficients by trying to obtain a maximum minimisation of the residual norm(s) [12, 14, 16].

4.2 Stabilisation: pseudotransient continuation

In some cases with a very strong mutual interaction, the relaxation is not sufficient. In this case a more elaborate technique, a stabilising pseudotransient continuation is required [17]. The steps of this approach consist of the solution of a transient problem converging smoothly to a

steady state, which is the desired coupled problem solution. Now, the rate of convergence is determined by the underlying thermal large time constant, which can be controlled.

Hence, the transient equation pair (3) and (7) is solved instead of the steady-state (4) and (5). The (pseudo-)time variable acts as continuation parameter. A more or less smooth converging evolution towards the nonlinear steady-state solution is pursued, by advancing the problem parameter t. This pseudo-time parameter can be interpreted as letting the solution slowly evolve towards the desired nonlinear solution point on a pseudo-timescale. Close to the steady state, where the time steps are large, the influence of the added time derivatives vanishes and the method converges towards the time-harmonic approach, the quasistationary solution.

A full transient approach, not using this envelope approach, is an alternative stabilisation technique. However, it is expensive to use because of the very short time-steps and it is more appropriate for irregular current excitations.

5 Algorithm comparison

5.1 Test problem

To compare the different nonlinear computational approaches the coupled FEM solution of a lean solid busbar operated at a voltage of 50 Hz is computed (Fig. 2). This test problem is representative for deep bars in an induction machine or an induction heating problem [18]. The electrical conductivity is temperature dependent. Here, the only losses in the model are Joule losses, caused by the source and the eddy currents in the conductor. The device is cooled by convection at all side faces. One edge is supposed to be cooled with a lower convection coefficient, introducing a moderately asymmetrical cooling, which can be an approximation to model rising cooling air due to natural convection.

The nonlinear coupled problem has (at least) two solutions. The first, physical, solution (Fig. 3) results in a moderate increase of the bar temperature, with the highest temperature at locations with the largest current density. The other solution is usually not feasible (Fig. 4). This can be a result of an unconstrained extrapolation of the material characteristics beyond the material's phase transformations. In this solution the current is concentrated on one side of the conductor where' as a consequence, a much higher temperature is encountered.

Whether the solution converges to the physical or nonphysical field depends on the algorithm, its parameters and the starting conditions. Convergence towards the

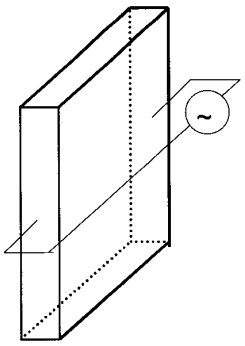

Fig. 2 *Coupled problem test model*

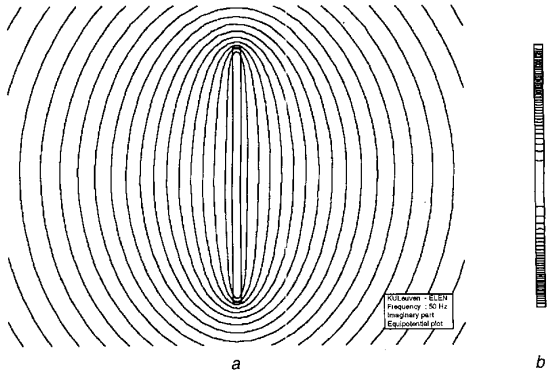

Fig. 3 *Magnetic and thermal field solution of coupled test problem ('correct physical solution')*
a. Magnetic field around bar.
b. Thermal field inside bar.

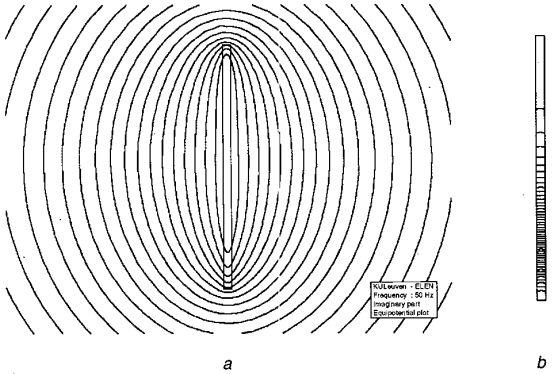

Fig. 4 *Magnetic and thermal field solution of coupled test problem ('incorrect physical solution': current has moved to one side and temperature distribution is extremely asymmetric)*
a. Magnetic field around bar.
b. Thermal field inside bar.

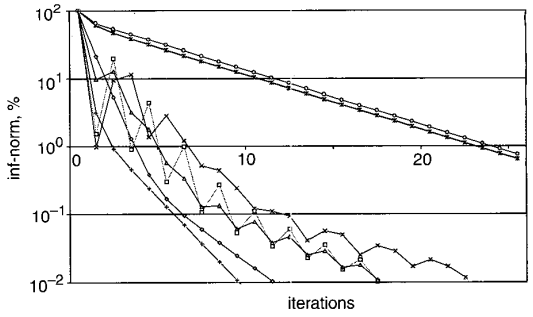

Fig. 5 *Comparison of convergence behaviour of model with low size ratio; all converge to 'physical solution'*
-◇- Block Gauss-Seidel
-□- Block Gauss-Seidel (relaxed)
-△- Block Jacobi
-×- Block Jacobi (relaxed)
-■- Time-Harmonic/Transient
-○- Transient Time-Harmonic/Transient
-x- Newton

nonphysical solution is more likely for conductors with a higher size ratio; Fig. 5 shows the smooth convergence behaviour of the ∞-norm for a low-size ratio model

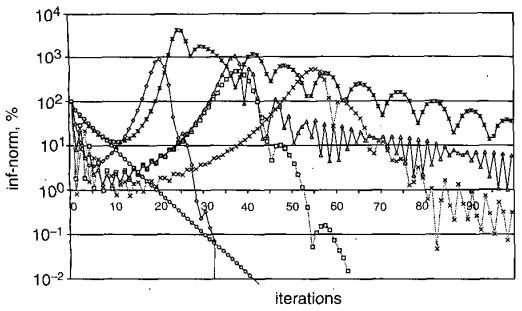

Fig. 6 *Comparison of convergence behaviour of model with high size ratio; all but pseudotransient algorithm converge to 'nonphysical solution'*
-◇- Block Gauss-Seidel
-□- Block Gauss-Seidel (relaxed)
-△- Block Jacobi
-×- Block Jacobi (relaxed)
-■- Time-Harmonic/Transient
-○- Transient Time-Harmonic/Transient

(neither relaxation nor stabilisation were necessary). This has to be compared with the irregular trends in Fig. 6 for a high size-ratio model, where many algorithms did not converge to the correct solution despite strong adaptive relaxation. For the high size-ratio model, the only algorithm converging to the physical solution was the pseudotransient algorithm based on the transient time-harmonic method (7). The Newton algorithm used for that computation was the described method with approximating jacobian–vector product in GMRES, that proved to be competitive when a good starting solution is available.

6 Discussion and algorithm choice

Though the previous discussion is built around a simplified magnetic–thermal coupled problem, the results can be used to predict the existence of convergence problems in coupled problems in a general way. As illustrated in [18], large practical problems such as foil-winding transformers show a similar convergence behaviour for the coupled-problem calculation methods outlined.

The reason why many algorithms diverge from a certain point in the test problem can be understood as follows. In this model significant current concentrations exist yielding loss concentrations. Therefore the temperature would increase at these locations as well, especially when cooling is not ideal. Due to these hot spots, the local material parameters change dramatically, linked with a totally different eddy current distribution, related losses and hot spots ... Mathematically, this causes intense oscillations and as a consequence the algorithms drift away from the correct solution.

Some important trends can be recognised in this simple model that can help to identify potentially difficult coupled electromagnetic–thermal problems:

- *The presence of nonuniform cooling mechanisms*: yielding asymmetrical heat transport paths as caused by local heat transport conditions or the shape of the conductor (e.g. high aspect ratios). The result is usually a significant temperature difference that can be destabilising.
- *The presence of nonuniform heat sources involving temperature-dependent loss mechanisms*: for instance, very concentrated skin effects yielding high locally losses. Others are concentrated iron loss, caused by fluxes that are indirectly influenced by temperature fluctuations. The 'harder' the nonlinear thermal dependence, the more severe the problems become.
- *Frequency dependence of the loss mechanism*, linked to the changing skin depth.

Table 1: Algorithm choice table for coupled electromagnetic–thermal problems

Method	*Advisable for*	*Remarks*
Block Jacobi	Problems with moderate risk	Parallelism capability
Block Gauss–Seidel	Problems with low risk	No parallelisation benefit
Steady-state time-harmonic/ transient	Not advisable, except when transient time harmonic method is not available	—
(Pseudo-) transient time-harmonic/ transient	Methods with high risk or any transient problem	Very robust
Full Newton	Problems that can be described by available simple differentiable functions	Nontrivial partial derivative calculation for jacobian causes high computational costs; ill-conditioned system
Quasi-Newton (approximate jacobian–vector product)	Problems requiring use of black-box solvers & for which good starting solutions exist	Very flexible, but the number of unknowns must be kept to minimum (GMRES memory consumption)

The presence of at least one of the discussed observations in a problem definition indicates that it should be handled with particular attention to the instabilities. It is advisable to try an initial solution with a 'safe' robust method and a fast 'dangerous' method to check whether a risk for nonphysical solutions or divergence exists. Table 1 may help in the selection of an appropriate effective and efficient algorithm.

7 Conclusion

Different nonlinear iterative-solution algorithms for coupled electromagnetic–thermal problems have been discussed and local as well as global convergence issues treated. The different approaches were compared using a test problem. This allows one to conclude that more robust algorithms such as pseudotransient continuation methods are required when significant skin effects in irregularly shaped conductors, possibly asymmetrically cooled, are present. Fast-converging Newton-type methods are often too expensive when compared with Picard methods, unless the quasi-Newton method approximating jacobian-vector products in iterative solvers can be used, for instance in the vicinity of the solution.

8 Acknowledgments

The authors are grateful to the Belgian "Fonds voor Wetenschappelijk Onderzoek Vlaanderen" for financial support of this work and the Belgian Ministry of Scientific Research for granting IUAP P4/20 on coupled problems in electromagnetic systems. The research council of K.U.

Leuven supported the basic numerical research. J. Driesen is a postdoctoral research fellow of the Belgian 'Fonds voor Wetenschappelijk Onderzoek Vlaanderen'.

9 References

1 WILLIAMSON, S., and LLOYD, M.R.: 'Cage rotor heating at standstill', *IEE Proc. B*, 1987, **134**, pp. 325–331
2 MOLFINO, P., and REPETTO, M.: 'Comparison of different strategies for the analysis of nonlinear coupled thermo-magnetic problems under pulsed conditions', *IEEE Trans. Magn.*, 1990, **26**, (2), pp. 559–562
3 CHABOUDEZ, C., CLAIN, S., GLARDON, R., RAPPAZ, J., SWIERKOSZ, M., and TOUZANI, R.: 'Numerical modelling of induction heating of long workpieces', *IEEE Trans. Magn.*, 1994, **30**, (6), pp. 5028–5037
4 FAGUNDES, J.C.S., BATISTA, A.J., and VIAROUGE, P.: 'Thermal modeling of pot core magnetic components used in high-frequency static converters', *IEEE Trans. Magn.*, 1997, **33**, (2), pp. 1710–1713
5 ORTEGA, J.M., and RHEINBOLDT, W.C.: 'Iterative solutions of nonlinear equations in several variables', (Academic Press, New York, 1970)
6 DRIESEN, J., and HAMEYER, K.: 'The simulation of magnetic problems with combined fast and slow dynamics using a transient time-harmonic method', *Eur. Phys. J.*, 2001, **13**, (3), pp. 165–169
7 FELDMANN, P., and ROYCHOWDHURY, J.: 'Computation of circuit waveform envelopes using an efficient, matrix-decomposed harmonic balance algorithm'. Proceedings of international conference on Computer aided design (ICCAD) '96, San Jose CA, USA, November 1996
8 KUNDERT, K.S.: 'Simulation methods for RF integrated circuits'. Proceedings of international conference on Computer aided design (ICCAD) '97, San Jose CA, USA, November 1997, pp. 752–765
9 ROYCHOWDHURY, J.: 'Efficient methods for simulating highly nonlinear multirate circuits'. Proceedings of conference on Design automation conference (DAC) '97, Anaheim CA, USA, June 1997, pp. 269–274
10 BEN-YAAKOV, S., GLOZMANN, S., and RABINOVICI, R.: 'Envelope simulation by SPICE-compatible models of linear electric circuits driven by modulated signals', *IEEE Trans. Ind. Appl.*, 2001, **37**, (2), pp. 527–533
11 DRIESEN, J., and HAMEYER, K.: 'Newton and quasi-Newton algorithms for nonlinear electromagnetic–thermal coupled problems'. Proceedings of EPNC'00, Krakow, Poland, September, pp. 7–10
12 JÄNICKE, L., and KOST, A.: 'Convergence properties of the Newton–Raphson method for nonlinear problems', *IEEE Trans. Magn*, 1998, **34**, (5), pp. 2505–2508
13 BARRETT, R. *et al.*: 'Templates for the solution of linear systems: Building blocks for iterative methods, (SIAM, 1984)
14 DENNIS, J.E., and SCHNABEL, R.B.: 'Numerical methods for unconstrained optimization and nonlinear equations', (SIAM, 1983)
15 BROWN, P.N.: 'A local convergence theory for combined inexact-Newton/finite difference projection methods', *SIAM J. Numer. Anal.*, 1987, **24**, (2), pp. 407–434
16 DRIESEN, J., BELMANS, R., and HAMEYER, K.: 'Adaptive relaxation algorithms for thermo-electromagnetic FEM problems', *IEEE Trans. Magn.*, 1999, **35**, (3), pp. 1622–1625
17 KELLEY, C.T., and KEYES, D.E.: 'Convergence analysis of pseudotransient continuation', *SIAM J. Numer. Anal.*, 1996, **35**, (2), pp. 508–523
18 DRIESEN, J.: 'Coupled electromagnetic–thermal problems in electrical energy transducers'. PhD Thesis, Faculty of Applied Sciences, K.U. Leuven, 2000